Journal Pre-proof

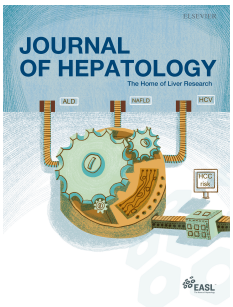

SARS-CoV-2 infection of the liver directly contributes to hepatic impairment in patients with COVID-19

Yijin Wang, Shuhong Liu, Hongyang Liu, Wei Li, Fang Lin, Lina Jiang, Xi Li, Pengfei Xu, Lixin Zhang, Lihua Zhao, Yun Cao, Jiarui Kang, Jianfa Yang, Ling Li, Xiaoyan Liu, Yan Li, Ruifang Nie, Jinsong Mu, Fengmin Lu, Shousong Zhao, Jiangyang Lu, Jingmin Zhao

PII: S0168-8278(20)30294-4

DOI: https://doi.org/10.1016/j.jhep.2020.05.002

Reference: JHEPAT 7747

To appear in: *Journal of Hepatology*

Received Date: 13 March 2020

Revised Date: 27 April 2020

Accepted Date: 3 May 2020

Please cite this article as: Wang Y, Liu S, Liu H, Li W, Lin F, Jiang L, Li X, Xu P, Zhang L, Zhao L, Cao Y, Kang J, Yang J, Li L, Liu X, Li Y, Nie R, Mu J, Lu F, Zhao S, Lu J, Zhao J, SARS-CoV-2 infection of the liver directly contributes to hepatic impairment in patients with COVID-19, *Journal of Hepatology* (2020), doi: https://doi.org/10.1016/j.jhep.2020.05.002.

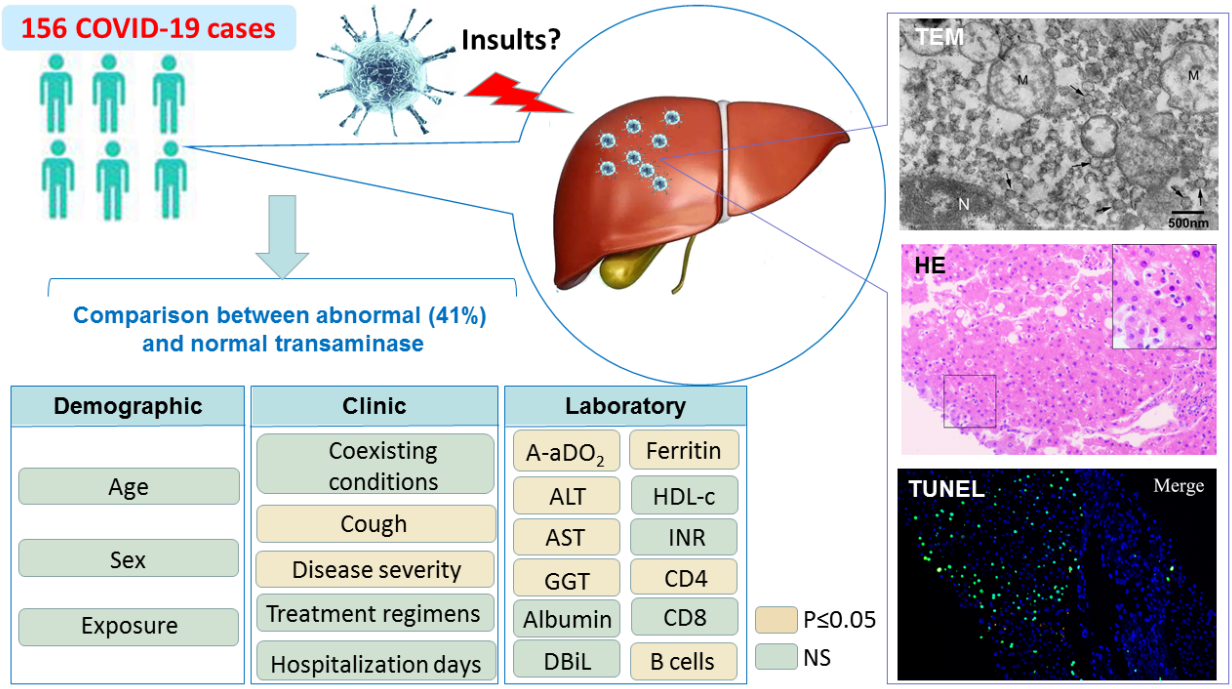

Demographic	Clinic	Laboratory		
Age	Coexisting conditions	A-aDO$_2$	Ferritin	P≤0.05
Sex	Cough	ALT	HDL-c	NS
Exposure	Disease severity	AST	INR	
	Treatment regimens	GGT	CD4	
	Hospitalization days	Albumin	CD8	
		DBiL	B cells	

SARS-CoV-2 infection of the liver directly contributes to hepatic impairment in patients with COVID-19

Yijin Wang[1#], Shuhong Liu[1#], Hongyang Liu[1#], Wei Li[2#], Fang Lin[3], Lina Jiang[1], Xi Li[1], Pengfei Xu[1], Lixin Zhang[1], Lihua Zhao[1], Yun Cao[2], Jiarui Kang[4], Jianfa Yang[1], Ling Li[1], Xiaoyan Liu[1], Yan Li[1], Ruifang Nie[1], Jinsong Mu[3], Fengmin Lu[5], Shousong Zhao[2], Jiangyang Lu[4], Jingmin Zhao[1]*

[1] Department of Pathology and Hepatology, The Fifth Medical Center of PLA General Hospital, Beijing, China

[2] Department of infectious diseases, First Affiliated Hospital of Bengbu Medical College, Bengbu, China

[3] Department of Intensive Care Unit, The Fifth Medical Center of PLA General Hospital, Beijing, China

[4] Department of Pathology, The Fourth Medical Center of PLA General Hospital, Beijing, China

[5] Department of Microbiology and Infectious Disease Center, School of Basic Medical Sciences, Peking University Health Science Center, Beijing, China

Correspondence to Dr. J. Zhao at Department of Pathology and Hepatology, The Fifth Medical Center of PLA General Hospital, No. 100 Xi Si Huan Middle Road, Beijing 100039, China, or at jmzhao302@163.com.

Drs. **Y. Wang**, **S. Liu, H. Liu** and **W. Li** contributed equally to this article.

Declaration of Interests: We declare that we have no conflicts of interest.

Declaration of submission: We declare that the paper has not been submitted to another journal, and has not been published in whole or in part elsewhere previously.

Financial support: None

Authors Contributions: JZ contributed to study concept and design, clinical and pathological analysis, study supervision and critical revision of the manuscript; YW contributed to study design, analysis and interpretation of data, literature search and writing of the manuscript; SL contributed to specimens collection and pathological and immunohischemical analysis; HL contributed to data analysis, making tables, and literature search; FL and JM contributed to clinical data analysis; WL, YC, LJ, XLi, XL and SZ contributed to clinical data collection; JL and JK contributed to electron microscope imaging and analysis; PX, LZ, JY, LL, YL contributed

to pathological and immunohischemical experiments; LZ contributed to making figures; RN contributed to literature search; CZ and JJ contributed to clinical data collection and analysis; FL contributed to data analysis.

Key words: COVID-19; Liver enzyme abnormality; SARS-CoV-2 infection; Cytopathy.

Word account: 5248

Number of figures and tables: 4

Abstract

Background: Liver enzyme abnormality is common in patients with coronavirus disease 2019 (COVID-19). Whether or not SARS-CoV-2 infection can lead to liver damage *per se* remains unknown. Here we reported the clinical characteristics and liver pathological manifestations of COVID-19 patients with liver enzyme abnormality.

Methods: We received 156 patients diagnosed of COVID-19 from two designated centers in China, and compared clinical features between patients with elevated aminotransferase or not. Postmortem liver biopsies were obtained from two cases who had elevated aminotransferase. We investigated the patterns of liver impairment by electron microscopy, immunohistochemistry, TUNEL assay, and pathological studies.

Results: 64 of 156 (41.0%) COVID-19 patients had elevated aminotransferase. The median levels of ALT were 50 U/L vs. 19 U/L, respectively, AST were 45.5 U/L vs. 24 U/L, respectively in abnormal and normal aminotransferase groups. The liver enzyme abnormality was associated with disease severity, as well as a series of laboratory tests including higher A-aDO2, higher GGT, lower albumin, decreased CD4+ T cells and B lymphocytes. Ultrastructural examination identified typical coronavirus particles characterized by spike structure in cytoplasm of hepatocytes in two COVID-19 cases. SARS-CoV-2 infected hepatocytes displayed conspicuous mitochondrial swelling, endoplasmic reticulum dilatation, and glycogen granule decrease. Histologically, massive hepatic apoptosis and a certain binuclear hepatocytes were observed. Taken together, both ultrastructural and histological evidence indicated a typical lesion of viral infection. Immunohistochemical results showed scanty CD4+ and CD8+ lymphocytes. No obvious eosinophil infiltration, cholestasis, fibrin deposition, granuloma, massive central necrosis, or interface hepatitis were observed.

Conclusions: SARS-CoV-2 infection in liver is a crucial cause of hepatic impairment in COVID-19 patients. Hence, a surveillance of viral clearance in liver and long outcome of COVID-19 is required.

Lay summary: Liver enzyme abnormality is common in patients with coronavirus disease 2019 (COVID-19). We reported the clinical characteristics and liver pathological manifestations of COVID-19 patients with elevated liver enzymes. Our findings suggested SARS-CoV-2 infection in liver is a crucial cause of hepatic impairment in COVID-19 patients

Introduction

Coronavirus disease 2019 (COVID-19) caused by severe acute respiratory syndrome coronavirus 2 (SARS-CoV-2) has spread globally, resulting in an ongoing pandemic. The epidemic outbreak of SARS-CoV-2 has caused more than 1.7 million confirmed infections and over 100 thousand fatal cases by April 11st, 2020, affecting 210 countries. Genetically, deep sequencing of lower respiratory tract samples characterizes the virus as a distinct clade from the betacoronaviruses associated with human severe acute respiratory syndrome (SARS) and Middle East respiratory syndrome (MERS) [1, 2]. The full spectrum of COVID-19 ranges from mild, self-limiting respiratory tract illness to severe progressive pneumonia. The common clinical manifestations of COVID-19 included elevated body temperature, dry cough, dyspnea, and no obvious improvement upon three days antibiotics treatment, as well as white blood cells decreasing and pulmonary infiltrate. However, the most additional striking feature extensively observed in these patients is liver enzyme abnormality that has been reported up to 50% of patients with COVID-19 and raise great clinical concern [3-5], despite SARS-CoV-2 is considered as a pneumophila virus. Whether or not the cytopathy of hepatocytes elicited by SARS-CoV-2 infection causes the liver impairment remains unknown.

In this study, we received 156 patients with COVID-19 from two designated centers and compared clinical features between abnormal and normal liver enzyme groups. Importantly, through histological, ultrastructural and immunohischemical examinations on biopsy liver tissues, we found that direct SARS-CoV-2 infection of the liver cells significantly contribute to the hepatic impairment in patients with COVID-19.

Methods

Patients and study design

Medical records of the patients diagnosed with COVID-19 from Jan 20 to Mar 25 from two COVID-19 designated centers in Beijing and Anhui province, China were reviewed. These patients were confirmed of SARS-CoV-2 infection by laboratory tests performed by Beijing Center for Disease Control and Prevention (Beijing CDC) and Anhui CDC. The diagnosis of COVID-19 was according to Guidelines issued by National Health Commission of China[6]. Only patients with SARS-CoV-2 infection as the only risk factor for liver injury were included

in this study. The exclusion criteria included co-infection with any viral hepatitis; presence of other chronic liver diseases (autoimmune hepatitis, primary biliary cholangitis, haemochromatosis and so forth); other viral pathogens co-infection, including influenza A/B, adenovirus, cytomegalovirus and Epstein-Barr virus; receiving long-term medication associated with liver dysfunction; having malignancy. We collected the patients' clinical data, including epidemiological, demographic, clinical, routine laboratory, radiology and treatment. Severe patients were diagnosed with the criteria that met at least one of the following conditions: (1) Shortness of breath, respiration rate ≥ 30 times/min, (2) Oxygen saturation (Resting state) ≤ 93%, or (3) PaO2 / FiO2 ≤ 300mmHg.

In order to identify clinical and laboratory features in COVID-19 patients with abnormal liver enzyme, the enrolled cases were designated into two groups of aminotransferase abnormality or not. Sustained alanine transaminase (ALT) or aspartate aminotransferase (AST) elevation over normal upper limit value (40 U/L) ≥ 7 days during disease course was defined as liver enzymes abnormality. For each patient, the peak value of ALT or AST among repeated liver function tests during hospitalization was selected for analysis, meanwhile other laboratory parameters obtained simultaneously were recorded. Meanwhile, in this study, liver function abnormality was regarded as abnormal ALT, AST, γ-glutamyl transferase (GGT), alkaline phosphatase (ALP), Albumin, direct bilirubin (DBiL), prothrombin time (PT) and INR. Liver synthetic dysfunction was defined as albumin below the lower limit of the normal range.

Two of the involved patients died of severe COVID-19. Both of them had aminotransferase derangement. After obtained informed consents, postmortem biopsies of lung and liver tissues were immediately obtained from them for pathological analysis according to regulations issued by the National Health Commission of China and the Helsinki Declaration.

Chest radiography evaluation

Chest radiographs obtained at the time in which patients have their peak ALT or AST were retrospectively reviewed and scored in consensus by three radiologists who were unaware of the clinical progress of the subjects. Scoring was according to the following criteria with 7 stages: 0, bilateral lungs showing clear textured; 1, bilateral lungs showing mild shadows; 2, single small patch shadow; 3, unilateral lung showing multiple patch shadow; 4, bilateral

lungs showing multiple patch shadow; 5, unilateral lung showing consolidation; 6, bilateral lung showing consolidation (less than 50%); 7, bilateral lung showing consolidation (more than 50%).

Specimen collection

SARS-CoV-2 diagnostic testing was in accordance with China CDC guidelines. Throat-swab specimens were obtained from patient and maintained in viral-transport medium stored between 2°C and 8°C until ready for shipment to the CDC. Lung and liver tissues were obtained by postmortem biopsied from two fatal patients.

Hematoxylin-Eosin (H&E) and immunohistochemistry (IHC) staining

Liver and lung specimens prepared for pathological examination were fixed with 4% neutral formaldehyde, embedded in paraffin wax, and 4 μm sections were cut. Sections were stained with haematoxylin and eosin (H&E).

Immunohistochemistry was used to determine the expression of CD68, CD4, CD8, and Ki67 in liver tissue. In detail, the liver biopsies were fixed in 10% formalin for 1.5 h at room temperature, processed for paraffin embedding, and sectioned at a thickness of 4 μm. The sections were incubated with monoclonal antibodies (CD4, CD8, Ki67 and were purchased from Zhongshan Golden Bridge Biotechnology, Beijing, China; CD68 was purchased from Maixin Biotech, Fuzhou, China) overnight at 4°C, and incubated with goat anti-mouse/rabbit secondary antibody (ZSGB-BIO,KIT-5030) for 15 min at 37°C. Subsequently, the sections were developed with diaminobenzidine (DAB) (ZSGB-BIO, ZLI-9018), followed by counterstaining hematoxylin. Immunostained sections were scanned using Leica DFC400 digital camera and Leica Application Suite software (Leica Microsystems).

Transmission Electron Microscope (TEM)

TEM was performed to observe ultrastructural changes and SARS-CoV-2 viral particles in liver tissue. In detail, liver biopsy specimens were immediately fixed with 2.5% glutaraldehyde and then postfixed with 1% osmium tetraoxide, dehydrated in a graded series of ethanol concentrations, and embedded in SPIPON812 resin. The ultrathin sections were sectioned with microtome (Leica EM UC6), approximately 70 nm, collected on copper grids and stained by uranyl acetate and lead citrate. Images were taken with a TEM

(JEM-1011 120kv).

Terminal deoxynucleotidyl transferase (TdT) dUTP NickEnd Labeling (TUNEL) assay

To detect cell apoptosis, TUNEL assay staining was performed following the manufactures' instructions. Paraffin-embedded section was prepared and stained with TUNEL reagents after sequential deparaffinization, followed by using an apoptosis in situ detection kit (Blue Skies, Shanghai, China). DAPI staining was used to count the total number of nuclei. TUNEL-positive cells labeled with fluorescein isothiocyanate were imaged by NIKON fluorescence microscopy. The frequency of apoptotic cells in liver section was semi-quantified by counting TUNEL positive cells in five microscopic fields per specimen.

Ethics approval

Samples collection and research on this case were exactly in accordance with regulations issued by the National Health Commission of China and the ethical standards formulated in the Helsinki Declaration. Written informed consent was obtained from patients with COVID-19 involved. The permission for retrospective study was obtained from the institutional review board of The Fifth Medical Center of PLA General Hospital and First Affiliated Hospital of Bengbu Medical College.

Statistical analysis

Results for continuous variables were expressed as mean ± standard deviation (SD) or median (interquartile range IQR), as appropriate. Categorical variables were presented as count (percentages). Differences between cases and controls were compared. Continuous variables were compared using Student t test or Mann-Whitney U test as appropriate. Categorical variables were compared using Chi-square or Fisher's exact test as appropriate. All statistical tests were two-sided and statistically significance was set at $p < 0.05$. Analyses were conducted with SAS 9.4 (SAS Institute, Cary, NC).

Results

Characteristics of COVID-19 patients with abnormal liver transaminases

A total of 156 COVID-19 patients were eligible for this study, including 54 severe cases and 102 non-severe cases, among which 64 (41.0%) had abnormal liver enzymes with an

elevated ALT being the most common abnormality described. Baseline demographic characteristics and clinical features, as well as treatment regimens of patients in two groups are reported in Table 1. They had a mean age of 51 years old in both groups and 82 (52.6%) were male with a similar sex ratio in both groups (59.4% and 47.8%, p = 0.580). In total, 96 (61.5%) cases are reported to either have a history in Hubei (endemic) or have an experience of close contact with confirmed COVID-19 patient, and there was no significant difference of the exposure history between the two groups. In addition, no significant differences were found with regard to coexisting medical conditions, including diabetes, hypertension, digestive system disease, endocrine system disease, nervous system disease, and chronic respiratory system disease between the two groups. The prevalence of initial symptoms were also similar in both groups except that COVID-19 patients with elevated liver enzymes had a greater proportion of cough (73.4% vs. 56.5, p = 0.031). Importantly, we found that liver transaminase abnormality was associated with disease severity (p = 0.007) and higher radiology scores (p = 0.007). Specifically, 30 of 54 (55.6%) severe cases and 24 of 102 (23.5%) non-severe cases presented elevated liver enzymes. Nine severe patients, including five of acute respiratory distress syndrome (ARDS), two of sepsis, one of acute kidney injury and one of uremia were admitted to intensive care unit (ICU), among which seven (77.8%) cases presented liver enzyme abnormality. The medication details of ICU patients, as well as their liver function tests were summarized in supplementary Table 1. In our study, all of the patients received antiviral therapy with PEG-Interferon α2b, Lopinavir/Ritonavir or both. Half of the patients were given antibiotic treatment and 26.3% patients were administered with systematic corticosteroids. Additionally, 26.9% patients were given immunoglobulin therapy. The treatment regimens were not significantly different between abnormal and normal transaminase groups. Of the 156 patients, the overall mortality was 2.6% (n = 4). Mortality occurred in three (4.7%) patients of liver enzymes abnormality (ARDS in two and septic shock in one) and one (1.1%) patient with normal liver enzymes (septic shock). The median duration of hospitalization was 19 days and 15 days (p = 0.127), respectively in patients with abnormal and normal liver enzymes.

Comparation of laboratory characteristics between COVID-19 patients with liver enzyme abnormality or not were surmised in Table 2. In term of arterial blood gas tests, the median values of alveolar-arterial oxygen tension difference (A-aDO_2) was dramatically higher in

patients with abnormal liver enzymes than those with normal liver enzymes (202.0 vs. 27.6, p = 0.022). Regard to liver enzyme tests, the median levels of ALT were 50.0 U/L and 19.0 U/L, respectively (p < 0.001), AST were 45.5 U/L and 24.0 U/L, respectively (p < 0.001) in patients with elevated and normal liver tests. Compared to patients with normal transaminases, patients who had elevated transaminase presented higher level of GGT while similar levels of ALP. In addition to liver enzymes, liver dysfunction as indicated by other common parameter abnormality, including lower albumin, higher DBiL, ferritin (FER) tended to be more frequent in patients with elevated liver enzymes than those with normal liver enzymes (p = 0.017, p = 0.058, p = 0.027). While the levels of total protein, globulin, and total bile acid (TBA) were normal and did not vary significantly between the two groups. Patients with abnormal liver enzymes showed elevated levels of lactate dehydrogenase (LDH), leucine aminopeptidase (LAP), urea nitrogen, creatine kinase, glucose and D-dimer. No significant differences of INR and PT were found between the two groups. The blood routine tests were comparable between the two groups except for higher values of both white blood cell (WBC) and absolute neutrophil (NEUT) counts in patients having elevated transaminases (p = 0.022 and p = 0.010), despite the median values were in normal ranges. While the total lymphocytes (455 vs. 891 /μl, p = 0.171), CD4+ lymphocytes (240 vs. 470 /μl, p = 0.024) and B lymphocytes (86 vs. 150 /μl, p = 0.025) in blood were all markedly decreased in abnormal transaminase group, although no statically significant difference for total lymphocytes. No significant differences of serum C-reactive protein, Interleukin-6 or procalcitonin were observed between two groups.

Liver histological and immunohistochemical findings

Case 1

Case 1 was a 50-year-old man presenting mild initial symptoms one week prior to admitting to hospital (day 8). He had a travel history to Wuhan before onset of symptoms. Interferon alfa-2b and lopinavir plus ritonavir were administered as antiviral therapy, and moxifloxacin was used to prevent secondary infection. However, the patient's symptoms did not ameliorated and his hypoxaemia and shortness of breath got worsen. On day 12, chest x-ray showed progressive infiltrate and diffuse gridding shadow in both lungs. His pulmonary function rapidly deteriorated and died of ARDS on day 14. He had elevated transaminases during the whole disease course with peak ALT and AST of 70 U/L and 111 U/L, respectively.

Histologic examination of lung tissue revealed diffuse alveolar damage (DAD), prominent desquamation of pneumocytes and hyaline membrane formation, indicating a severe acute lung injury (Fig. 1A). Liver biopsy showed substantial cluster or scattered apoptotic hepatocytes characterized by condensed nuclear or formed apoptotic body (Fig. 1B). Prominent binuclear or occasional multinuclear syncytial hepatocytes were identified. No obvious viral inclusions were identified. There were moderate micro- and mild macro-vesicular steatosis. Other pathologic manifestation included mild to moderate focal lobular inflammation with infiltration of predominant lymphocytes and few neutrophils. Mild inflammation in portal tract with lymphocytic infiltrate was occasionally identified. There was no eosinophil infiltration, cholestasis, granuloma, fibrin deposition, centrilobular necrosis, or interface hepatitis.

Immunohistochemistry revealed increased CD68+ cells mainly distributed in hepatic sinusoids (50-60 positive cell counts per 200X power field), suggesting Kupffer cells activation (Fig. 1C). CD4+ cells were infrequently presented (3-5 positive cell counts per 400X power field) (Fig. 1D). A few CD8+ cells were scattered in liver lobule and portal areas (5-15 positive cell counts per 400X power field) (Fig. 1E). There were some Ki-67 positive cells in hepatocytes and infiltrated mononuclear cells (8-10 positive cell counts per 400X power field) (Fig. 1F).

TUNEL positive cells with green florescence in nucleus indicated apoptotic cells. Liver tissue of peri-hemangioma from one hepatic hemangioma case was used for control (Fig. 1G-I). The number of apoptotic hepatocytes was remarkably abundant in liver of COVID-19 patient (80-120 positive cell counts per 200X power field) compared with that in control liver (5-8 positive cell counts per 200X power field) (Fig. 1G-L).

Ultrastructurally, TEM examination identified amounts of typical coronavirus particles with spike structure in cytoplasm of hepatocytes, most viral particles exist without membrane-bound vesicles (Fig. 1M). The virions were round, mildly pleomorphic, and showed surface thickening envelop indicative of the corona peplomer structure, with size ranges between 60-120 nm. Intriguingly, SARS-CoV-2 infected hepatocyte exhibited markedly swelling mitochondria with obscure cristae or high electronic density materials, strongly indicating SARS-CoV-2 directly caused cytopathy. Moderate density fat was observed and glycogen granules were apparently decreased in hepatocytes.

Case 2

Case 2 was a 79-year old female admitted to hospital with repeated febrile, fatigue, dizziness, myalgia, and cough. She reported a close contact with her daughter who had SARS-CoV-2. Despite receiving antiviral and antibacterial medications, her situation became worsen and developed respiratory failure and hemorrhagic shock on day 11 and day 18, respectively. SARS-CoV-2 RNA test was still positive on day 24. On Illness Day 26, she suddenly developed chills and hyperpyrexia. Chest X-ray images showed a rapid deterioration of pneumonia. *Klebsiella pneumoniae* was identified in both blood and sputum samples. This patient died of septic shock on day 28. Her liver enzymes increased gradually during the last few days with peak ALT and AST of 76 and 236 U/L.

The lung pathological feature indicated late phase DAD and loose interstitial fibrosis with admixed areas of fibrinous exudation and edema in alveolar space (Fig. 2A). Liver biopsy showed quite similar histology to the case 1 with conspicuous multi-focal or scanty apoptotic bodies (Fig. 2B). There were plenty of binuclear or occasional multinuclear cells with apparent nucleolus and congregated chromatin. Moderate micro- and mild macro-vesicular steatosis were also observed. The portal inflammation was very mild. No centrilobular necrosis, ductular/canalicular cholestasis, venalities, interface hepatitis, or haemophagocytosis were identified.

Immunohistologically, numerous CD68+ cells with larger size were seen predominantly in sinusoids (150-200 counts per 200X power field) (Fig. 2C). Scattered CD4+ and CD8+ cells appeared in lobules (Fig. 2D-E). There were some Ki67 positive cells in hepatocytes and Kupffer cells (5-10 positive cell counts per 400X power field) (Fig. 2F).

TUNEL assay displayed plenty of apoptotic hepatocytes in this patient (60-120 positive cell counts per 200X power field), comparable with that in case 1 (Fig. 2G-I)

TEM showed numerous coronavirus particles with size range between 70-120 nm in cytoplasm without membrane-bound vesicles in hepatocytes (Fig. 2J). The majority of viral particles were intact but a few fragmented virions were also visible. High electronic density lipid droplets were noted. The pattern of cell damage included glycogen granule decrease in hepatocytes and canalicular impairment with shedding of microvilli, suggesting a cytopathic lesion caused by SARS-CoV-2 infection.

Discussion

Coronaviruses have a broad host range and cause a wide variety of respiratory, gastrointestinal, and systemic diseases in animals and humans. Liver enzyme abnormalities developed in as many as 50% of SARS-CoV-2 infected patients reported by varied studies. In our study, 41.0% COVID-19 patients presented liver enzyme abnormality, and the prevalence was 23.5% even in the context of mild cases, confirming liver impairment is common in COVID-19 patients. The liver enzyme abnormality was associated with disease severity, as well as a series of laboratory tests, including higher A-aDO_2, higher FER, lower albumin, and decreased circulating CD4+ T cells and B lymphocytes. Importantly, we firstly provided the direct evidence of SARS-CoV-2 infection, rapid replication and evident cytopathy of hepatocytes, suggesting direct SARS-CoV-2 infection in liver is one of causes of liver impairment in COVID-19 patients, though other factors such as drug toxicity or complication insults to liver could not be excluded.

SARS-CoV in 2002–2003 outbreak has also been reported to cause liver impairment [7, 8]. However, the evidence of visible coronavirus particles under TEM in liver tissue was lacked [9, 10]. In this study, abundant SARS-CoV-2 viral particles were observed in cytoplasm of hepatocytes in two COVID-19 cases. The majority of viral particles were noted to harbor completed envelope with corona-like spikes, indicating SARS-CoV-2 is not only able to entry, but also replicate in hepatocytes. Strikingly, ultrastructural features of conspicuous mitochondria swelling, endoplasmic reticulum dilatation, and impaired cell membrane demonstrated a cytopathy of SARS-CoV-2 in hepatocytes. Moreover, massive hepatic apoptosis and binuclear or a few multinuclear hepatocytes, which were syncytial, rather than proliferative identified by Ki67 IHC, were the predominant histological features of viral infection. Meanwhile, IHC results showed scanty CD4+ and CD8+ cells in liver tissues, suggesting immunopathologic insult might not be involved in liver damage. Taken together, histological and ultrastructural evidences indicated that SARS-CoV-2 dissemination in liver potentially contributed to abnormal liver transaminases.

Angiotensin-converting enzyme 2 (ACE2) is known as cell entry receptor of both SARS-CoV and SARS-CoV-2 [2, 11]. SARS-CoV-2 is perceived to be unfavorable in liver infection due to less ACE2 expression in hepatocytes. However, we found abundant SARS-CoV-2 viral

particles in hepatocytes. Usually, the receptor distribution is considered to be concordant with that of infected organs. Nevertheless, there exist notable discordances of ACE2 expression in SARS-CoV targeted multiorgans [12, 13], such as virus replication in colonic epithelium, which has no ACE2, and no virus infection in endothelial cells, which have ACE2 [14]. These discrepancies suggested the localization of ACE2 does not fully explain the liver tropism of SARS-CoV-2. We speculated alternative extra-ACE2 receptors or co-receptors might exist. Another possibility is that the expression of ACE2 in hepatocytes may be up-regulated upon sensing virus entry. We however have no data on the expression of ACE2 in SARS-CoV-2 infected liver and further study is required to address this hypothesis.

One of the striking observations in our study was that the A-aDO_2 was dramatically higher in patients with liver transaminase abnormality, implying the liver damage may amenable to poor pulmonary function in COVID-19 patients. Mechanistically, proinflammatory cytokines were reported to increase significantly in severe COVID-19 cases [4, 15]. This event often provokes systemic ischemia and hypoxia blamed for inadequate pulmonary ventilation, which manifested in elevation of A-aDO_2. Thus severe COVID-19 patients may predispose to develop hypoxic-ischemic liver injury. The hallmark of ischemic liver injury is centrilobular necrosis and usually identified by acute and marked increase of serum transaminase [16, 17]. The two biopsied cases in the current study however did not present the pathological feature of ischemic liver and their serum transaminases were increased moderately, implicating the liver impairment in these two cases might be independent of pulmonary dysfunction to extent. Additionally, other COVID-19 related complications could not be ruled out involved in liver enzyme abnormality, such as sepsis. There were only two septic patients in our study, one with elevated liver enzyme (case 2) and one being of normal liver enzyme, implicating sepsis is unlikely a factor that contribute to the high rate of liver enzyme abnormality in the current cohort. Additionally, the pathological examination in case 2 showed no septic pathological features of centrilobular necrosis, canalicular/ductular cholestasis, non-bacterial cholangitis, suggesting sepsis insult is unlikely a main cause of liver impairment in this case. Nevertheless, due to the limited septic patients in our cohort, we could not provide convincing data on the frequency of liver function abnormality in septic patients.

Drug induced liver injury (DILI) might be an alternative insult of liver damage. According to

our results, no significant differences in terms of antiviral and antibiotic medications were found between normal and abnormal liver enzyme groups. Moreover, as hepatotoxicity usually occurs after long-term antiviral therapy, the clinical courses of our patients did not favor antiviral drug induced liver injury. Indeed, hepatotoxicity may occur in the first few weeks after antibiotic therapy and typically related to remarkable elevation of liver enzymes, sometimes in conjunction with allergic reactions such as rash. However, our patients had no such obvious adverse reaction, and the media ALT level was 50 (40.0-70.0) in this cohort. Histologically, although both SARS-CoV-2 infection and drug might result in liver steatosis [18-20], the pathological features of no obvious eosinophil infiltration, cholestasis, fibrin deposition, granuloma, massive central necrosis, or interface hepatitis in the two biopsied cases were not complying with DILI. Nevertheless, we could not exclude DILI as a participating cause since the two biopsied cases were unable to represent the entire cohort.

Several other laboratory variables were identified to associate with transaminases abnormality of COVID-19. The median GGT values in both groups of abnormal and normal transaminase were in normal rangeand no significant differences in levels of direct bilirubin (DBiL), total bilirubin (TBiL), or alkaline phosphatase (ALP) were observed between two groups, suggesting bile ducts were unlikely the SARS-CoV-2 target sites. Notably, patients with elevated liver enzymes were more frequent to have lower serum albumin, suggesting an association of liver synthetic dysfunction and liver enzyme abnormality in COVID-19 patients. Serum FER level was higher in patients with elevated transaminase. Physiologically, one third FER was stored in liver and the circulating FER is normally able to be cleared by the liver cells. Therefore patients with damaged liver may fail to get rid of circulating FER, leading to an accumulated FER in serum. Immune disruption, characterized by lymphopenia, decreased levels of CD4+ T cells and B lymphocytes, was more profoundly in transaminases elevated cases. However, the serum IL-6 was not higher, but even lower in patients with abnormal transaminase. Besides, both lymphopenia and elevated liver enzymes were linked to severity of COVID-19. We thereafter assumed that the immune dysfunction and liver impairment were coincident events, rather than cause-effect relationship.

There were limitations in our study. Due to barely accessible autopsy or biopsy, we have only two biopsied cases for ultrastructural and pathological analysis, which were unable to represent the entire cohort. Moreover, the cohort is not larger enough and limited to two

centers. Therefore, large- and multi-cohort studies that contain more cases available for biopsy or autopsy were justified to comprehensively understand liver impairment in COVID-19 patients. However, we believe that our remarkable findings offered crucial clue to liver enzyme abnormality in COVID-19 patients.

In this study, we identified the clinical and laboratory characteristics of COVID-19 patients with abnormal liver transaminases and firstly reported SARS-CoV-2 is able to infect liver and cause liver impairment of conspicuous cytopathy. In this perspective, a surveillance of viral clearance in liver and long outcome of COVID-19 is required. Additional researches on how and to what extent that SARS-COV-2 infection involved in liver enzyme abnormality in distinct COVID-19 population are required.

References

[1] Zhu N, Zhang D, Wang W, Li X, Yang B, Song J, et al. A Novel Coronavirus from Patients with Pneumonia in China, 2019. N Engl J Med 2020.

[2] Zhou P, Yang XL, Wang XG, Hu B, Zhang L, Zhang W, et al. A pneumonia outbreak associated with a new coronavirus of probable bat origin. Nature 2020.

[3] Xu XW, Wu XX, Jiang XG, Xu KJ, Ying LJ, Ma CL, et al. Clinical findings in a group of patients infected with the 2019 novel coronavirus (SARS-Cov-2) outside of Wuhan, China: retrospective case series. BMJ 2020;368:m606.

[4] Huang C, Wang Y, Li X, Ren L, Zhao J, Hu Y, et al. Clinical features of patients infected with 2019 novel coronavirus in Wuhan, China. Lancet 2020.

[5] Chen N, Zhou M, Dong X, Qu J, Gong F, Han Y, et al. Epidemiological and clinical characteristics of 99 cases of 2019 novel coronavirus pneumonia in Wuhan, China: a descriptive study. Lancet 2020.

[6] New coronavirus pneumonia prevention and control program (5th ed.) (in Chinese). 2020.

[7] Lee N, Hui D, Wu A, Chan P, Cameron P, Joynt GM, et al. A major outbreak of severe acute respiratory syndrome in Hong Kong. N Engl J Med 2003;348:1986-1994.

[8] Tsang KW, Ho PL, Ooi GC, Yee WK, Wang T, Chan-Yeung M, et al. A cluster of cases of severe acute respiratory syndrome in Hong Kong. N Engl J Med 2003;348:1977-1985.

[9] Chau TN, Lee KC, Yao H, Tsang TY, Chow TC, Yeung YC, et al. SARS-associated viral hepatitis caused by a novel coronavirus: report of three cases. Hepatology 2004;39:302-310.

[10] Poutanen SM, Low DE, Henry B, Finkelstein S, Rose D, Green K, et al. Identification of severe acute respiratory syndrome in Canada. N Engl J Med 2003;348:1995-2005.

[11] Li W, Moore MJ, Vasilieva N, Sui J, Wong SK, Berne MA, et al. Angiotensin-converting enzyme 2 is a functional receptor for the SARS coronavirus. Nature 2003;426:450-454.

[12] Hamming I, Timens W, Bulthuis ML, Lely AT, Navis G, van Goor H. Tissue distribution of ACE2 protein, the functional receptor for SARS coronavirus. A first step in understanding SARS pathogenesis. J Pathol 2004;203:631-637.

[13] Cheung OY, Chan JW, Ng CK, Koo CK. The spectrum of pathological changes in severe acute respiratory syndrome (SARS). Histopathology 2004;45:119-124.

[14] Chen J, Subbarao K. The Immunobiology of SARS*. Annu Rev Immunol 2007;25:443-472.
[15] Chen G, Wu D, Guo W, Cao Y, Huang D, Wang H, et al. Clinical and immunologic features in severe and moderate Coronavirus Disease 2019. J Clin Invest 2020.
[16] Henrion J, Schapira M, Luwaert R, Colin L, Delannoy A, Heller FR. Hypoxic hepatitis: clinical and hemodynamic study in 142 consecutive cases. Medicine (Baltimore) 2003;82:392-406.
[17] Seeto RK, Fenn B, Rockey DC. Ischemic hepatitis: clinical presentation and pathogenesis. Am J Med 2000;109:109-113.
[18] Bessone F, Dirchwolf M, Rodil MA, Razori MV, Roma MG. Review article: drug-induced liver injury in the context of nonalcoholic fatty liver disease - a physiopathological and clinical integrated view. Aliment Pharmacol Ther 2018;48:892-913.
[19] Gordon A, McLean CA, Pedersen JS, Bailey MJ, Roberts SK. Hepatic steatosis in chronic hepatitis B and C: predictors, distribution and effect on fibrosis. J Hepatol 2005;43:38-44.
[20] Nishida N, Chiba T, Ohtani M, Yoshioka N. Sudden unexpected death of a 17-year-old male infected with the influenza virus. Leg Med (Tokyo) 2005;7:51-57.

Figure legends

Fig. 1 Postmortem biopsy specimens from case 1. (A) Lung tissue showing diffuse alveolar damage, desquamation and hyaline membrane, and multinucleated syncytial pneumocytes, as well as interstitial mononuclear infiltrates (H&E staining, original magnification ×200, up-right region original magnification ×400). (B) Liver tissue showing substantial apoptotic hepatocytes, prominent binuclear hepatocytes, and mild to moderate steatosis. (H&E staining, original magnification ×200, up-right region original magnification ×400). (C) Immunohistochemistry of liver tissue revealing activated CD68+ cells (original magnification ×200), (D) scattered CD4+ cells and (E) CD8+ cells in lobular and portal areas (original magnification ×400). (F) Nuclear proliferative antigen Ki-67 was positive in a few mononuclear cells and hepatocytes (original magnification ×400). TUNEL staining (green) showing apoptotic cells in control liver tissue (G-I) and in COVID-19 liver tissue (J-L). DAPI (blue) was applied to visualize nuclei. (M) Ultrastructural examination identifying amounts of typical coronavirus particles (arrow) with size of 60-120nm in cytoplasm of hepatocytes. Ultrastructural impairment manifesting conspicuous mitochondria (marked as M) swelling and glycogen granule decrease (original magnification ×15000).

Fig. 2 Postmortem biopsy specimens from case 2. (A) Lung tissue showing late phase diffuse alveolar damage, with cellular and fibrinous exudation, hemorrhage and foamy cells in alveolar space (H&E staining, original magnification ×400). (B) Liver tissue revealing

abundant apoptotic hepatocytes, plenty of binuclear cells, and mild to moderate micro- and macro-vesicular steatosis (H&E staining, original magnification ×200). (C) Immunohistochemistry of liver tissue revealing numerous activated CD68+ Kupffer cells (original magnification ×200), (D) scattered CD4+ and (E) CD8+ cells in lobule (original magnification ×400). (F) A few Ki67 positive proliferative hepatocytes and Kupffer cells (original magnification ×400). (G-I) TUNEL assay displaying apoptotic hepatocytes (green). (J) Electron microscopy showing numerous coronavirus particles (arrow) in cytoplasm of hepatocytes. The pattern of cell damage including decreased glycogen granules and canalicular (marked as C) impairment with shedding of microvilli (original magnification×12000).

- Liver enzyme abnormality in COVID-19 patients is associated with disease severity.
- COVID-19 patients with liver enzyme abnormality have higher A-aDO2, higher GGT, lower albumin and decreased circulating CD4+ T cells and B lymphocytes.
- SARS-CoV-2 is able to infect liver and cause conspicuous hepatic cytopathy.
- Massive apoptosis and binuclear hepatocytes were the predominant histological features of SARS-CoV-2 infected liver.

Table 1 Demographic and clinical characteristics*

Characteristics	Patients with abnormal transaminase N = 64	Patients with normal transaminase N = 92	*P*
Age (year)	51.1 ± 17.4	51.2 ± 15.2	0.962
Sex			
Male	38 (59.4)	44 (47.8)	0.155
Female	26 (40.6)	48 (52.2)	
Exposure			
Hubei province exposure	20 (31.3)	25 (27.2)	0.580
Close contact with COVID-19 patient	21 (32.8)	41 (44.6)	0.140
All of the above	5 (7.8)	6 (6.5)	1.000
No exposure	28 (43.8)	32 (34.8)	0.258
Coexisting medical conditions			
Diabetes	9 (14.1)	8 (8.7)	0.290
Hypertension	20 (31.3)	22 (23.9)	0.310
Digestive system disease	1 (1.6)	5 (5.4)	0.402
Endocrine system disease	1 (1.6)	2 (2.2)	1.000
Nervous system disease	2 (3.1)	2 (2.2)	1.000
Chronic respiratory system disease	4 (6.3)	4 (4.4)	0.717
Other underlying disease	-	-	-
Signs and symptoms			
Fever	60 (93.8)	83 (90.2)	0.432
Cough	47 (73.4)	52 (56.5)	0.031
Myalgia or fatigue	18 (28.1)	34 (37.0)	0.250
Sputum production	22 (34.4)	26 (28.3)	0.416
Headache	10 (15.6)	14 (15.2)	0.945
Haemoptysis	1 (1.6)	2 (2.2)	1.000
Diarrhoea	6 (9.4)	12 (13.0)	0.481
Dyspnoea	12 (18.8)	22 (23.9)	0.442
Sore throat	7 (10.9)	17 (18.5)	0.199
Rhinorrhoea	2 (3.1)	1 (1.1)	0.568
Chest pain	3 (4.7)	2 (2.2)	0.401
Nausea and vomiting	1 (1.6)	4 (4.4)	0.649
Severe patients	30 (46.9)	24 (26.1)	0.007
Radiology scores[#]			0.007
0-3	33.3%	66.7%	
4-7	66.7%	33.3%	
Treatment			
PEG-Interferon α2b	59 (92.2)	85 (92.4)	1.000
Lopinavir/Ritonavir	38 (59.4)	57 (62.0)	0.745
Antibiotic treatment	33 (51.6)	40 (43.5)	0.320
Use of corticosteroid	20 (31.3)	21 (22.8)	0.240
Intravenous immunoglobulin therapy	19 (29.7)	23 (25.0)	0.516
Mortality	3 (4.7)	1 (1.1)	0.306
Hospitalization days	19 (14-24)	15 (12-23)	0.127

* Normally distributed continuous variables were expressed in mean ± standard deviation (SD), whereas other continuous variables were expressed in median (interquartile range [IQR]). Categorical variables were presented as counts (percentage). Qualitative and quantitative

differences between 2 groups were analyzed by Chi-square test or Fisher exact test for categorical parameters and Student t test or Mann-Whitney U test for continuous parameters as appropriate. Levels of significance: $p < 0.05$.

Data of chest scores were available in 27 patients with abnormal transaminase and 42 patients with normal transaminase, respectively.

Table 2 Laboratory characteristics*

Variables	Patients with abnormal transaminase N = 64	Patients with normal transaminase N = 92	*P*
Arterial blood gas			
PO_2 80-100 (mmHg)	83.5 (79.5-92.0)	92.0 (80.0-126.0)	0.341
TCO_2 23-27 (mmol/L)	24.9 (23.9-28.6)	27.0 (26.2-28.4)	0.325
CL 93-100 (mmol/L)	104 (99-106)	103 (100-105)	0.617
Anion gap 23-65 (mmol/L)	12.0 (9.1-15.8)	12.6 (11.3-16.9)	0.443
SaO_2 95-100 (%)	96 (96-97)	97 (96-99)	0.344
A-aDO_2 10-15 (mmHg)	202.0 (30.5-331.2)	27.6 (15.2-37.7)	0.022
O_2Cont 7.5-23 (vol%)	17.3 (15.1-18.8)	18.8 (17.4-20.4)	0.088
P50 25-29 (mmHg)	25.7 (25.2-26.9)	26.7 (25.3-28.8)	0.323
Lactic acid 0.6-2.2 (mmol/L)	2.1 (1.8-2.4)	2.0 (1.5-2.9)	0.559
Biochemical tests			
Liver enzymes			
ALT 5-40 (U/L)	50.0 (40.0-70.0)	19.0 (14.6-28.5)	< 0.001
AST 5-40 (U/L)	45.5 (38.0-60.0)	24.0 (19.7-29.0)	< 0.001
AST/ALT	0.89 (0.60-1.36)	0.96 (0.72-1.38)	0.498
ALP 40-150 (U/L)	61 (49-76)	63 (48-76)	0.842
GGT 11-50 (U/L)	45 (28-78)	22 (15-40)	< 0.001
Ratio of abnormality	45%	22%	0.002
Liver function			
Total protein 60-83(g/L)	68 (63-73)	69 (64-73)	0.773
Albumin 35-55(g/L)	37 (33-41)	39 (36-41)	0.067
Ratio of abnormality	38.1%	20.7%	0.017
Globumin 20-40(g/L)	32 (28-35)	30 (27-33)	0.097
TBiL 3.4-20.5 (μmol/L)	10.5 (8.2-15.4)	9.5 (7.1-15.4)	0.286
Ratio of abnormality	14%	13%	0.855
DBiL 0-6.8 (μmol/L)	3.6 (2.4-6.4)	3.1 (1.8-5.3)	0.141
Ratio of abnormality	23%	12%	0.058
TBA 0-10 (μmol/L)	3.0 (1.9-5.9)	2.6 (1.4-3.8)	0.185
Ferritin 30-400 (ng/ml)	632.7 (339.1-1128.0)	300.0 (95.3-429.8)	< 0.001
Ratio of abnormality	68%	40%	0.027
Other biochemical tests			
Lactate dehydrogenase 109-245 (U/L)	279 (218-399)	218 (187-271)	< 0.001
Adenosine deaminase 0-20 (U/L)	17.1 (12.0-24.9)	13.7 (11.0-20.2)	0.059
Cholinesterase 5000-12000 (U/L)	7221 (5522-8016)	7151 (5987-8211)	0.405
Leucine aminopeptidase 39-80 (U/L)	61 (50-68)	49 (42-56)	0.007
Blood urea nitrogen 2.9-8.2 (mmol/L)	4.7 (3.8-5.6)	3.7 (3.2-4.5)	0.004
Creatine kinase 26-140 (U/L)	81.5 (42.0-232.5)	54.0 (36.0-88.0)	0.004
Creatinine 62-115 (μmol/L)	66.5 (50.7-79.5)	67.5 (55.6-80.5)	0.781
Uric acid 208-428 (μmol/L)	231 (174-316)	234 (175-301)	0.654
Glucose 3.9-6.1 (mmol/L)	6.0 (5.2-8.0)	5.3 (4.8-6.3)	0.005
Total cholesterol 2.8-5.2 (mmol/L)	3.8 (3.2-4.4)	3.9 (3.5-4.5)	0.443

Triglyceride 0.56-1.7 (mmol/L)	1.15 (0.93-1.74)	1.20 (0.92-1.69)	0.652
HDL-c 1.29-1.55 (mmol/L)	0.96 (0.83-1.19)	1.00 (0.83-1.23)	0.447
LDL-c 2.1-3.1 (mmol/L)	2.37 (2.01-3.01)	2.40 (1.90-2.96)	0.903
Apolipoprotein A1 1.05-2.05 (g/L)	0.91 (0.74-1.03)	1.00 (0.79-1.14)	0.049
Apolipoprotein B 0.55-1.30 (g/L)	0.85 (0.66-1.07)	0.77 (0.64-0.95)	0.238
Lipoprotein (a) 0-300 (mg/L)	184 (62-303)	180 (101-352)	0.668
Coagulation function			
INR 0.8-1.2	1.05 (1.00-1.10)	1.05 (0.99-1.10)	0.329
Prothrombin time 10.2-14.3 (sec)	12.1 (11.5-12.6)	11.8 (11.3-12.5)	0.223
D-dimer < 0.55 (mg/L)	0.53 (0.24-1.10)	0.37 (0.22-0.68)	0.032
Blood routine			
WBC 3.97-9.15 (10^9/L)	5.7 (4.5-8.2)	5.2 (3.9-6.6)	0.022
NEUT 2-7 (10^9/L)	3.90 (2.61-5.72)	3.10 (2.19-4.01)	0.010
LYMPH 0.8-4.0 (10^9/L)	1.20 (0.75-1.86)	1.40 (1.15-1.81)	0.090
Absolute monocyte 0.12-1.0 (10^9/L)	0.46 (0.27-0.59)	0.38 (0.28-0.55)	0.194
Absolute eosinophil 0.02-0.5 (10^9/L)	0.02 (0.01-0.11)	0.07 (0.01-0.12)	0.183
absolute basophilic 0-1 (10^9/L)	0.02 (0.01-0.03)	0.01 (0.01-0.03)	0.278
RBC 4.09-5.74 (10^{12}/L)	4.27 (3.85-4.71)	4.34 (3.86-4.70)	0.579
ESR 0-15 (mm/60min)	32.9 (17.0-59.0)	23.8 (10.0-51.5)	0.326
Haemoglobin 131-172 (g/L)	129 (118-144)	131 (120-141)	0.655
PCV 38-50.8 (%)	39.0 (35.7-42.6)	39.0 (35.3-42.5)	0.742
MCV 83.9-99.1 (fL)	91.6 (87.1-95.5)	91.4 (88.0-94.7)	0.789
MCHC 27.8-33.8 (pg)	30.4 (29.0-31.7)	30.4 (29.2-31.5)	0.988
RDW 0-15 (%)	13.2 (12.5-44.3)	13.1 (12.5-40.8)	0.230
PLT 85-303 (10^9/L)	186 (139-250)	199 (155-252)	0.319
PCT 0.06-0.40 (%)	0.21 (0.16-0.25)	0.22 (0.17-0.28)	0.220
MPV 7.54-11.24 (fL)	9.5 (8.4-10.6)	9.7 (8.8-10.7)	0.611
PDW 9.0-18.0 (%)	14.0 (11.8-15.9)	12.5 (11.1-15.8)	0.099
P-LCR 13-43 (%)	26.5 (23.2-33.4)	26.1 (22.3-31.4)	0.490
Lymphocytes			
T LYMPH 690-2540 (/μl)	455 (303-1358)	891 (631-1045)	0.171
CD4 LYMPH 410-1590 (/μl)	240 (106-606)	470 (344-616)	0.024
CD8 LYMPH 190-1140 (/μl)	236 (116-531)	367 (228-509)	0.241
B LYMPH 90-660 (/μl)	86 (51-174)	150 (107-196)	0.025
NK LYMPH 90-590 (/μl)	124 (51-186)	161 (122-221)	0.051
CD4/CD8 0.68-2.47	1.20 (0.79-1.67)	1.20 (0.95-1.63)	0.537
Infection related biomarkers			
C-reactive protein 0.068-8.2 (mg/L)	19.5 (3.2-57.6)	9.8 (2.4-35.2)	0.156
Interleukin-6 (pg/ml)	4.7 (1.9-13.7)	7.1 (3.7-16.4)	0.255
Procalcitonin 0-0.5 (ng/ml)	0.04 (0.02-0.09)	0.04 (0.02-0.06)	0.290

* Normally distributed continuous variables were expressed in mean ± standard deviation (SD), whereas other continuous variables were expressed in median (interquartile range [IQR]). Categorical variables were presented as percentage. Qualitative and quantitative differences between 2 groups were analyzed by Chi-square test or Fisher exact test for categorical parameters as appropriate and Mann-Whitney U test for continuous parameters. Levels of significance: $p < 0.05$.

Abbreviations: PO_2, oxygen partial pressure; TCO_2, total carbon dioxide; K, potassium; Cl, chlorine; SaO, oxygen saturation; A-aDO_2, alveolar-arterial oxygen partial pressure difference; O_2Cont, oxygen content of blood; P50, oxygen half-saturation pressure of hemoglobin; ALT,

alanine aminotransferase; AST, aspartate aminotransferase; ALP, alkaline phosphatase; GGT, γ-glutamyl transferase; TBiL, total bilirubin; DBiL, direct bilirubin; INR, international normalized ratio; PT, Prothrombin time; TBA, total bile acid; HDL-c, high density lipoprotein cholesterol; LDL-c, low density lipoprotein cholesterol; WBC, white blood cell; NEUT, absolute neutrophil count; LYMPH, absolute lymphocyte value; RBC, red blood cell; PCV, packed cell volume; MCV, mean corpuscular volume; MCHC, mean corpuscular hemoglobin concentration; RDW, red cell distribution with; PLT, platelet count; PCT, platelet cubic measure distributing; MPV, mean platelet volume; PDW, platelet distribution width; P-LCR, platelet-large cell ratio; NK, natural killer cell; ESR, erythrocyte sedimentation rate.

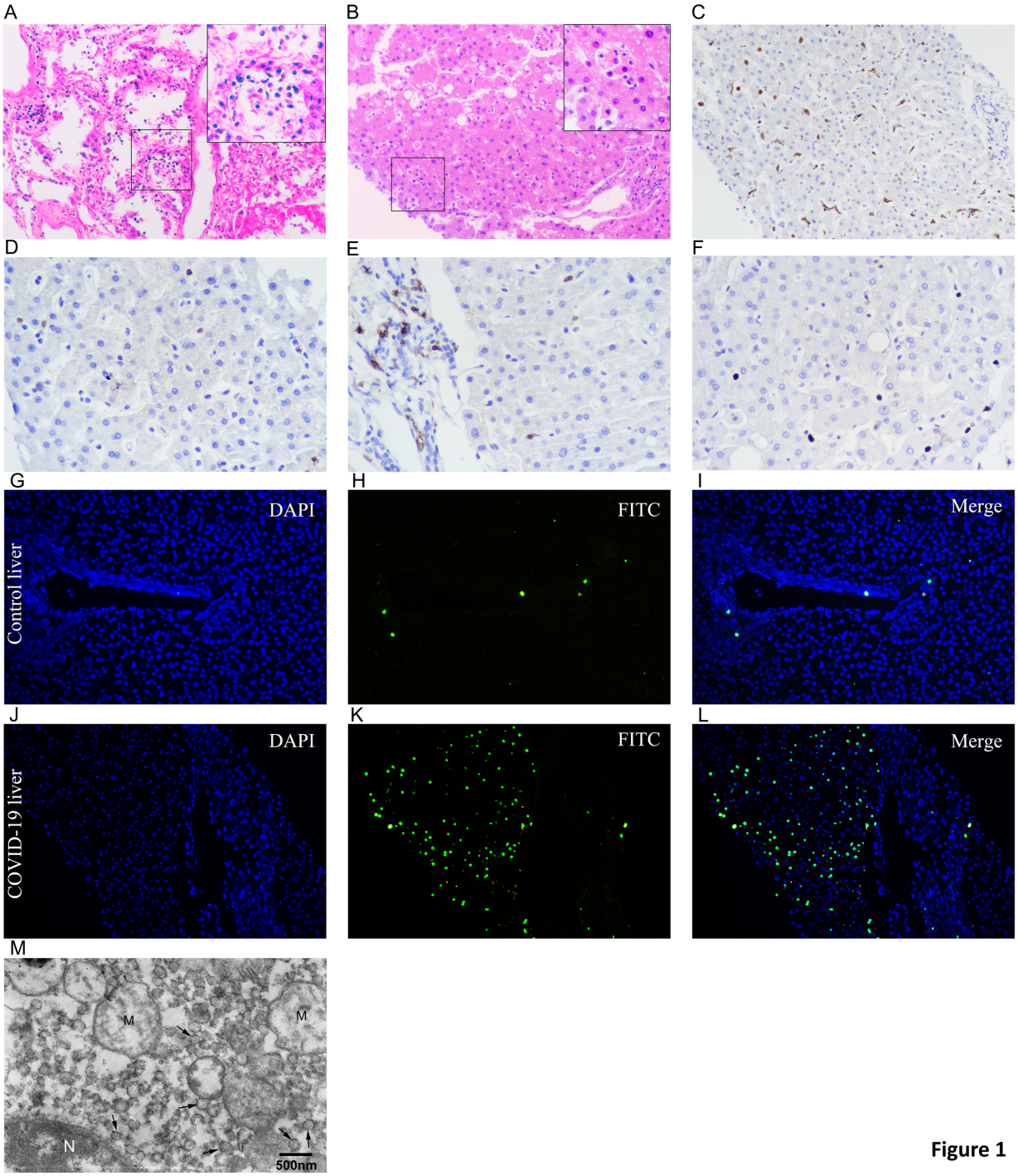
A
B
C
D
E
F
G
DAPI
Control liver
H
FITC
I
Merge
J
DAPI
COVID-19 liver
K
FITC
L
Merge
M
M
M
N
500nm

Figure 1

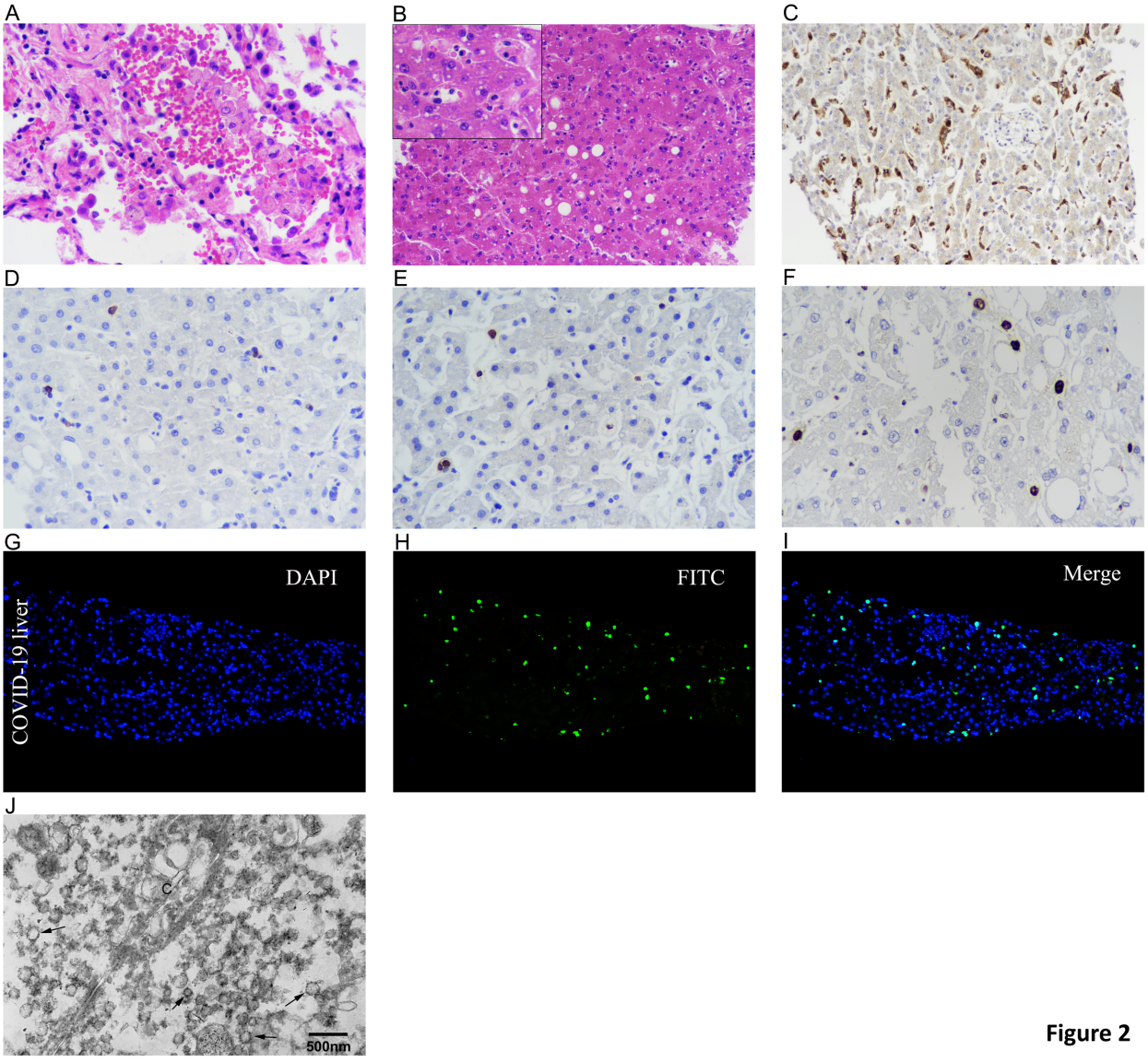

Figure 2